

Adaptive local thresholding can enhance the accuracy of HR-pQCT-based trabecular bone morphology assessment

Citation for published version (APA):

Mys, K., Stockmans, F., Gueorguiev, B., Wyers, C. E., van den Bergh, J. P. W., van Lenthe, G. H., & Varga, P. (2022). Adaptive local thresholding can enhance the accuracy of HR-pQCT-based trabecular bone morphology assessment. *Bone*, 154, Article 116225. <https://doi.org/10.1016/j.bone.2021.116225>

Document status and date:

Published: 01/01/2022

DOI:

[10.1016/j.bone.2021.116225](https://doi.org/10.1016/j.bone.2021.116225)

Document Version:

Publisher's PDF, also known as Version of record

Document license:

Taverne

Please check the document version of this publication:

- A submitted manuscript is the version of the article upon submission and before peer-review. There can be important differences between the submitted version and the official published version of record. People interested in the research are advised to contact the author for the final version of the publication, or visit the DOI to the publisher's website.
- The final author version and the galley proof are versions of the publication after peer review.
- The final published version features the final layout of the paper including the volume, issue and page numbers.

[Link to publication](#)

General rights

Copyright and moral rights for the publications made accessible in the public portal are retained by the authors and/or other copyright owners and it is a condition of accessing publications that users recognise and abide by the legal requirements associated with these rights.

- Users may download and print one copy of any publication from the public portal for the purpose of private study or research.
- You may not further distribute the material or use it for any profit-making activity or commercial gain
- You may freely distribute the URL identifying the publication in the public portal.

If the publication is distributed under the terms of Article 25fa of the Dutch Copyright Act, indicated by the "Taverne" license above, please follow below link for the End User Agreement:

www.umlib.nl/taverne-license

Take down policy

If you believe that this document breaches copyright please contact us at:

repository@maastrichtuniversity.nl

providing details and we will investigate your claim.



Adaptive local thresholding can enhance the accuracy of HR-pQCT-based trabecular bone morphology assessment

Karen Mys^{a,b,*}, Filip Stockmans^c, Boyko Gueorguiev^b, Caroline E. Wyers^{d,e}, Joop P. W. van den Bergh^{d,e,f}, G. Harry van Lenthe^a, Peter Varga^b

^a Biomechanics Section, Mechanical Engineering, KU Leuven, Leuven, Belgium

^b AO Research Institute Davos, Davos, Switzerland

^c Muscles & Movement, Department of Development and Regeneration, KU Leuven Campus Kulak, Kortrijk, Belgium

^d Department of Internal Medicine, VieCuri Medical Center, Venlo, the Netherlands

^e NUTRIM School for Nutrition and Translational Research in Metabolism, Maastricht University, Maastricht, the Netherlands

^f Department of Internal Medicine, Subdivision of Rheumatology, Maastricht University Medical Centre, Maastricht, the Netherlands

ABSTRACT

High-resolution peripheral quantitative computed tomography (HR-pQCT) devices can scan extremities at bone microstructural level *in vivo* and are used mainly in research of bone diseases. Two HR-pQCT scanners are commercially available to date: XtremeCT (first generation) and XtremeCT-II (second generation) from Scanco Medical AG (Switzerland). Recently, we have proposed an adaptive local thresholding (AT) technique and showed that it can improve quantification accuracy of bone microstructural parameters, with visually less sharp cone-beam CT (CBCT) images providing a similar accuracy than XtremeCT. The aim of this study was to evaluate whether the AT segmentation technique could enhance the accuracy of HR-pQCT in quantifying bone microstructural images and to assess whether the agreement between XtremeCT and XtremeCT-II could be improved.

Nineteen radii were scanned with three scanners from Scanco Medical AG: (1) XtremeCT at 82 μm , (2) XtremeCT-II at 60.7 μm and (3) the small animal microCT scanner VivaCT40 at 19 μm voxel size. The scans were segmented applying two different methods, once following the manufacturer standard technique (ST), and once by means of AT. Three-dimensional (3D) morphological analysis was performed on the trabecular volume of the segmented images using the manufacturer's standard software to calculate bone volume fraction (BV/TV), trabecular thickness (Tb.Th), separation (Tb.Sp) and number (Tb.N).

The average accuracy of XtremeCT improved from $R^2 = 0.76$ (ST) to 0.85 (AT) and reached the same level of accuracy as XtremeCT-II with ST ($R^2 = 0.86$). The largest improvements were obtained for BV/TV and Tb.Th. For XtremeCT-II, mean accuracy improved slightly from $R^2 = 0.86$ (ST) to 0.89 (AT). For both segmentations and both scanners, the standard section was quantified slightly more accurate than the subchondral section. The agreement between the scanners was enhanced from $R^2 = 0.89$ (ST) to 0.98 (AT).

In conclusion, AT can enhance the accuracy of XtremeCT to quantify distal radius bone microstructural parameters close to XtremeCT-II level and increases the agreement between the two HR-pQCT scanners.

High-resolution peripheral quantitative computed tomography, segmentation, bone microstructural parameters.

1. Introduction

Imaging of bones and joints is an essential part of the investigation of diseases that affect bone structure, such as osteoporosis and osteoarthritis [1,2]. High-resolution peripheral computed tomography (HR-pQCT) is considered the best technique to scan bone at high-resolution *in vivo* [3]. Currently, two HR-pQCT scanners are commercially available. The first-generation HR-pQCT scanner, XtremeCT (Scanco Medical AG, Brüttisellen, Switzerland), is able to acquire *in vivo* images at 82 μm voxel size (resolution < 130 μm). The second generation HR-pQCT scanner, XtremeCT-II (Scanco), enables scanning at 60.7 μm voxel size

(resolution < 90 μm) *in vivo* [4] and provides accurate, direct assessment of bone volume fraction on the segmented images and evaluation of trabecular microstructure *via* distance transform [5–7]. In contrast, the resolution of XtremeCT is considered to be at the limit for directly quantifying bone microstructure. Therefore, an indirect evaluation approach is applied, where trabecular bone mineral density (BMD) is taken to predict bone volume fraction, ridge extraction is applied to measure trabecular number (Tb.N), and a plate model is used to estimate other trabecular measures [3,8–10]. Direct measures of bone microstructural parameters are advantageous because they do not rely on the plate assumption and provide results independent of trabecular BMD.

* Corresponding author.

E-mail address: karen.mys@aofoundation.org (K. Mys).

<https://doi.org/10.1016/j.bone.2021.116225>

Received 23 May 2021; Received in revised form 28 September 2021; Accepted 28 September 2021

Available online 9 October 2021

8756-3282/© 2021 Elsevier Inc. All rights reserved.

Due to the indirect quantification technique, the accuracy of the XtremeCT is lower than XtremeCT-II, especially for trabecular thickness (Tb.Th) [5], and there is no good correlation between the scanners for this parameter [11].

Image segmentation is an essential part of the process of microstructural measurements. The standard evaluation protocols of HR-pQCT devices are referred to here as standard techniques (ST). For XtremeCT-II, a classic amplitude segmentation utilizing a global threshold is combined with a prior Gaussian filter having a small kernel to decrease noise. As the resolution of XtremeCT is close to the trabecular thickness, more advanced segmentation techniques are needed to compensate for the partial volume effect [12] and therefore an edge-enhancing Laplace-Hamming filtering is applied prior to a global thresholding.

In a previous study, we proposed an adaptive local thresholding segmentation technique (AT) [13,14] for cone-beam computed tomography (CBCT) [15]. The current state of the art CBCT scanners have a lower resolution (voxel size of 75 μm and resolution of <278 μm for

NewTom 5G, Cefla, Italy) than HR-pQCT and the images appear visually less sharp. Nevertheless, by applying AT on CBCT data, the reported accuracy of quantifying bone microstructural parameters of radii was similar to XtremeCT, with the standard analysis techniques being used for the latter [16]. Similar results were observed in another study on human trapezia where higher accuracy was obtained for CBCT with AT compared to the standard Laplace-Hamming edge detecting segmentation technique used for XtremeCT [14]. Based on these encouraging results on CBCT images, we hypothesized that the AT technique could enhance the accuracy of HR-pQCT in quantifying trabecular microarchitecture.

Therefore, the aims of this study were (1) to investigate whether AT improves the accuracy of XtremeCT and XtremeCT-II compared with the scanner-specific ST segmentation techniques for quantification of trabecular bone microstructural parameters in human distal radii *ex vivo*, considering the results of a microCT scanner as ground truth, and (2) to assess whether the agreement between XtremeCT and XtremeCT-II improves when using AT instead of the ST, which is of interest for

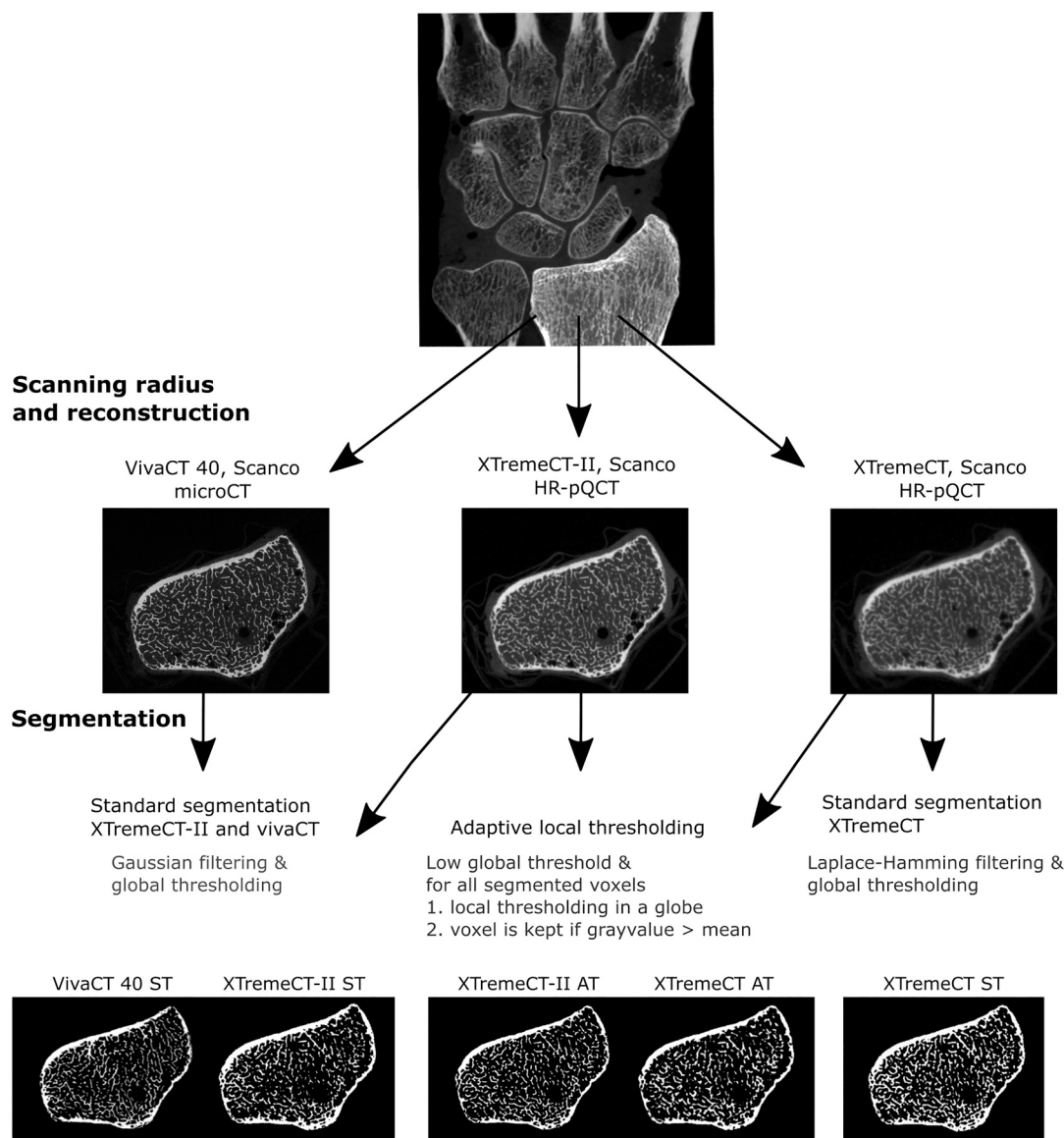


Fig. 1. Overview of the methodology in the current study. First, the radii were scanned with the microCT scanner VivaCT40 (Scanco Medical AG, Switzerland) and with both HR-pQCT scanners (XtremeCT and XtremeCT-II, Scanco Medical AG, Switzerland). All scans were reconstructed with the manufacturer's software. The microCT images were segmented as advised by the manufacturer. The HR-pQCT images were segmented twice; once with the standard technique (ST) applying standard segmentation provided by the manufacturer, and once with adaptive local thresholding technique (AT).

multicentre studies.

2. Materials & methods

2.1. Sample collection and scanning

The AT technique was applied on 9 mm long sections of the human distal radius, which is the most often investigated anatomical site with HR-pQCT [4]. The sample set and scanning technique were described in previous work [13,16]. In short, nineteen fresh-frozen human radii (14 females and 5 males; 8 left and 11 right) with donor age ranging from 25 to 93 years (67.9 ± 16.2 years; mean \pm standard deviation (SD)) were obtained from Science Care (Phoenix, AZ, USA) with appropriate informed consent of the donors. The distal parts of the radii were scanned with three different scanners: (1) XtremeCT, at a voxel size of $82 \mu\text{m}$, (2) XtremeCT-II, at a voxel size of $60.7 \mu\text{m}$ and (3) a small-animal microCT scanner (VivaCT40, Scanco Medical AG, Switzerland) at a voxel size of $19 \mu\text{m}$ (Fig. 1). MicroCT was used as the gold standard in all further analyses. Embedding of the shaft region and custom adapters allowed reproducible and centralized sample positioning in the different scanners. Two 9 mm sections were imaged and evaluated for each bone (Fig. 2). The first section, termed ‘subchondral section’ throughout this work, was located adjacent to the most proximal point of the subchondral endplate and aligned perpendicular to the longitudinal axis line of the scan. The second section, termed ‘standard section’, started directly distal to the subchondral section and mimicked the measurement area recommended for clinical scanning [10,16]. The subchondral region, which is in general harder to quantify accurately, has been shown to be more representative for actual bone strength than the standard region [17,18]. This study focused on the trabecular bone

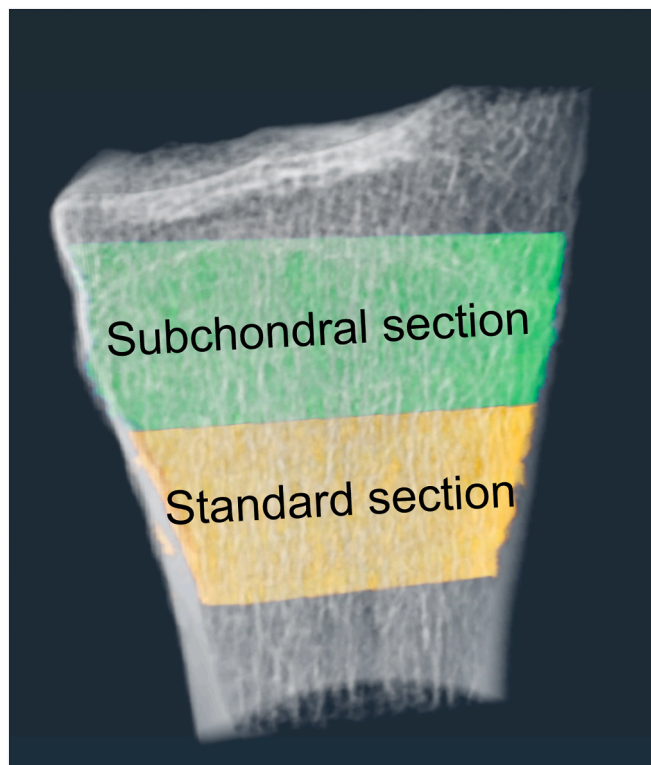


Fig. 2. Two 9 mm sections were imaged and evaluated for each bone. The first section, termed ‘subchondral section’ throughout this work, is located adjacent to the most proximal point of the subchondral endplate and aligned perpendicular to the longitudinal axis line of the scan and is indicated in green. The second section, termed ‘standard section’, starts directly distal to the subchondral section and mimicked the measurement area recommended for clinical scanning and is indicated in yellow.

regions of both sections.

2.2. Image segmentation

All HR-pQCT images were segmented with two different techniques (Fig. 1). First, the manufacturer’s software (IPL, Scanco Medical AG, Brüttisellen, Switzerland) was used to apply the ST technique according to the standard protocols of XtremeCT and XtremeCT-II, respectively. Second, AT was used for the segmentation via an in-house developed software implemented in C++.

The AT implementation was a simplified version of the original algorithm developed for CBCT images [13] where two segmentations were performed in parallel and combined afterwards. As originally the first segmentation – applying a local adaptive threshold to obtain an accurate detailed trabecular structure – tended to be inaccurate for thick structures such as the cortical bone, a second segmentation used a high global threshold to select the thick bone structures not appropriately captured by the first adaptive thresholding. However, as only the trabecular bone compartment was evaluated in the current study, the second segmentation was not necessary, and the used AT technique in this study only applied a global pre-segmentation with a low threshold value and a subsequent local adaptive thresholding within a spherical region having a diameter of 6 voxels. The local adapted threshold was set as the mean of minimum and maximum values in the actual region. As no HR-pQCT-specific parameters were available for AT, in analogy with our previous study on CBCT [16], the value of the low global threshold was optimized in steps of 5 mg HA/ccm to maximize the accuracy (R^2) of the results of all parameters and separately for Tb.Th. No optimisation was done to minimize the bias or the offset. To avoid over-fitting of the parameters, the stability of the optimisation was tested over multiple random subsamples. This test showed that the chosen parameters were reasonable and stable over those subsamples (data not shown). The microCT images were segmented according to the manufacturer’s ST protocol using Gaussian filtering followed by global thresholding.

The trabecular bone compartment of the distal radius was identified automatically on the microCT images utilizing an extended method based on the approach originally proposed by Buie et al. [19], as described elsewhere [13]. The same VOI was selected on the HR-pQCT images by registering them to the microCT-images in Amira (v6.2, Thermo Fisher Scientific, USA). To avoid loss of resolution of the gray-scale images due to resampling, the mask of the VOI determined on the microCT images was rotated by the inverse transformation and applied on the HR-pQCT images.

2.3. Calculation trabecular bone microstructural parameters

For the ST-based analysis, the microstructural parameters were calculated for all three scanners in the trabecular volume of interest (VOI) according to the manufacturer standard protocols using the IPL software (Scanco Medical AG, Brüttisellen, Switzerland). Accordingly, indirect quantification was used for XTremeCT and direct quantification was applied for both XTremeCT-II and microCT. For AT, direct quantification procedure of the XTremeCT-II was used for both HR-pQCT scanners. The evaluated parameters included bone volume fraction (BV/TV), Tb.Th, trabecular separation (Tb.Sp) and Tb.N.

2.4. Statistics

Statistical analyses were performed in Matlab R2017b (The Mathworks, USA) and R v4.0.2 (R Foundation for Statistical Computing, Austria). Quantification accuracy was evaluated for each microstructural parameter by performing linear regression analyses of XtremeCT and XtremeCT-II against microCT; the relative offset and the coefficient of determination (R^2) were calculated. Offset was calculated as the average difference compared to the microCT-based value. Statistical significance was evaluated at 5 and 10% level between the dependent

correlations with Williams's and Steiger's twotailed test [20]. Normality of the distribution was checked with the one-sample Kolmogorov-Smirnov test.

3. Results

3.1. Optimization of the AT threshold

The optimal value of the (low) global threshold of AT for XtremeCT was found to be 280 mg HA/ccm for Tb.Th and 190 mg HA/ccm for BV/TV, Tb.Sp and Tb.N. For XtremeCT-II, the optimal AT threshold was closely the same for all bone parameters and was therefore fixed to 240 mg HA/ccm.

3.2. XtremeCT

The AT-segmented images provided better quantification accuracy (R^2) for all microstructural parameters compared to the ST and improved the results of XtremeCT approaching the level of XtremeCT-II. The mean R^2 of XtremeCT increased from 0.76 (ST) to 0.85 (AT); mean R^2 of XtremeCT-II ST was = 0.86 (Fig. 3, Table 1).

This improvement was mainly due to an increased accuracy for BV/TV and Tb.Th. Tb.Sp and Tb.N were in general similar for both segmentations (difference in $R^2 \leq 0.04$). The only advantage of ST was observed for Tb.Sp. Both segmentation techniques were able to quantify the standard section slightly better than the subchondral section (Table 1).

3.3. XtremeCT-II

The standard ST technique was able to quantify bone parameters in XtremeCT-II with high accuracy (mean $R^2 = 0.86$). AT provided slightly

improved results (mean $R^2 = 0.89$, Fig. 4, Table 1). For the subchondral section Tb.Sp, a significant improvement was observed with AT. The standard section was in general quantified slightly more accurately compared to the subchondral section for both segmentations also for this scanner.

3.4. Agreement between XtremeCT and XtremeCT-II

The agreement between the bone microstructure parameters of both scanners increased by using AT (mean $R^2 = 0.98$) instead of ST (mean $R^2 = 0.89$, Fig. 5, Table 2). This was mainly due to the significantly improved quantification of Tb.Th.

4. Discussion

This study demonstrated that the accuracy of HR-pQCT for quantification of bone microstructural parameters could be enhanced when using an adaptive segmentation technique. These improvements were achieved without altering the hardware or scanning protocols of the scanners.

With this modified segmentation technique, it was possible to enhance the accuracy of the XtremeCT for microstructural evaluation in the distal radius from a mean R^2 of 0.76 (ST) to 0.85 (AT). Considering that the mean R^2 for XtremeCT-II with ST was 0.86, this implies that the modified segmentation is able to enhance the accuracy of XtremeCT closely to the level of XtremeCT-II. In more detail, AT improved the accuracy of BV/TV and Tb.Th. The two other parameters, namely Tb.Sp and Tb.N did not improve for XtremeCT, which is not surprising, as ST already provided an accuracy similar to that of XtremeCT-II (R^2 is 0.04 smaller at most). At the same time, by using the AT segmentation technique, it became possible to evaluate the bone microstructural parameters based on XtremeCT images using the direct method, which has

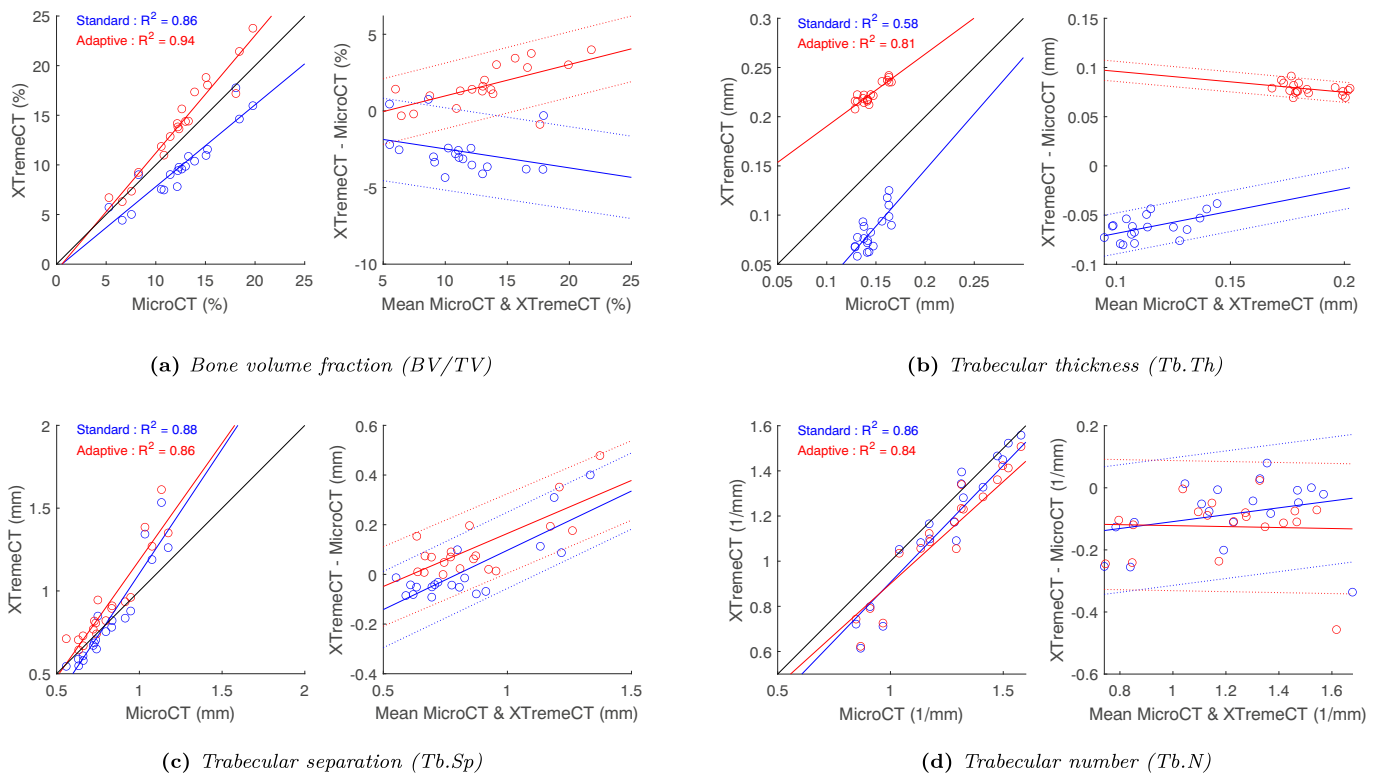


Fig. 3. Scatter plots and Bland Altman plots between MicroCT and XtremeCT for the standard region for (a) bone volume fraction (BV/TV), (b) trabecular thickness (Tb.Th), (c) trabecular separation (Tb.Sp) and (d) trabecular number (Tb.N). The XtremeCT images were segmented twice: once with the standard software recommended by the manufacturer, referred to as ST, and once with the proposed segmentation technique in this study – adaptive local thresholding – referred to as AT. The solid line on the scatter plot indicates a perfect match with $y = x$.

Table 1

Relative offset, bias, slope and coefficient of determination (R^2) of the linear regression analyses shown for XtremeCT and XtremeCT-II with respect to microCT. The offset was calculated as the average difference compared to the microCT-based value. Two segmentations techniques were used for both XtremeCT and XtremeCT-II: the standard software recommended by the manufacturer – referred to as ST – and the proposed segmentation technique in this study – adaptive local thresholding – referred to as AT. Statistically significant differences between the correlation strength achieved with AT versus ST are indicated as follows: ** Significantly improved at 5%. * Significantly improved at 10%.

		XtremeCT							
		ST				AT			
		Rel. offset	Bias	Slope	R^2	Rel. offset	Bias	Slope	R^2
Subchondral	BV/TV	-27.75	-1.65	0.83	0.88	17.92	-2.18	1.32	0.93
	Tb.Th	-43.12	-0.05	0.94	0.45**	56.72	0.12	0.73	0.86**
	Tb.Sp	-6.30	-0.16	1.17	0.82	7.22	-0.03	1.12	0.78
	Tb.N	-4.44	0.04	0.93	0.75	-6.13	0.12	0.85	0.75
	Average	-20.40			0.73	18.93			0.83
Standard	BV/TV	-20.74	-0.45	0.83	0.86	12.67	-0.64	1.18	0.94
	Tb.Th	-43.02	-0.08	1.14	0.58*	54.29	0.12	0.73	0.81*
	Tb.Sp	-0.25	-0.40	1.50	0.88	-2.57	-0.23	1.41	0.86
	Tb.N	-7.43	-0.13	1.03	0.86	-10.19	0.00	0.90	0.84
	Average	-17.86			0.80	13.55			0.86
	Average all				0.76				0.85

		XtremeCT-II							
		ST				AT			
		Rel. offset	Bias	Slope	R^2	Rel. offset	Bias	Slope	R^2
Subchondral	BV/TV	7.85	-5.84	1.46	0.96	4.79	-1.52	1.15	0.97
	Tb.Th	44.59	0.04	1.15	0.84	26.06	0.09	0.62	0.89
	Tb.Sp	15.90	-0.07	1.26	0.75**	8.13	-0.07	1.18	0.84**
	Tb.N	-14.45	0.07	0.81	0.75	-8.13	0.09	0.85	0.78
	Average	13.47			0.83	7.71			0.87
Standard	BV/TV	9.47	-1.84	1.25	0.94	4.60	-0.05	1.05	0.97
	Tb.Th	42.36	0.04	1.12	0.85	25.71	0.10	0.54	0.89
	Tb.Sp	18.47	-0.31	1.58	0.88	17.65	-0.30	1.50	0.89
	Tb.N	-15.81	-0.06	0.90	0.88	-11.11	-0.06	0.94	0.87
	Average	13.62			0.89	9.21			0.91
	Average all				0.86				0.89

as advantage of being independent of trabecular BMD [5].

For XtremeCT-II, the accuracy obtained for the bone microstructural parameters with the standard ST segmentation was already high (average $R^2 = 0.89$ and 0.83 for the standard and subchondral section, respectively). Compared to ST, AT provided a slight increase in the correlations to 0.91 and 0.87 , respectively. Here, the main improvement was obtained for the parameters Tb.Th and Tb.Sp.

To be able to compare results in multicentre studies between sites having different HR-pQCT generations, it is important to ensure agreement between different scanners. Manske et al. demonstrated that XtremeCT and XtremeCT-II scanners provided highly comparable results for bone microstructural parameters except Tb.Th ($R^2 = 0.51$) [11]. Their findings are well in line with the similar results obtained for the standard ST segmentation in the current study. However, when AT was used, the overall agreement between the two scanners increased from $R^2 = 0.91$ to 0.98 and from 0.87 to 0.98 for the standard and subchondral sections, respectively. The largest improvement was achieved for Tb.Th, with a correlation coefficient becoming significant higher, 0.93 and 0.95 with AT instead of 0.74 and 0.62 with ST for the standard and subchondral sections, respectively.

The improvement of AT for XtremeCT-II was apparently small. However, the main advantage is not the marginal enhancement when using the second generation HR-pQCT scanner with the high-resolution setting, but rather the possibility of delivering almost similarly accurate bone microstructural parameters based on a lower resolution image, allowing to decrease scanning time and radiation dosage, e.g. using the XTremeCT protocol of the XTremeCT-II scanner. The latter is particularly interesting to alleviate motion artefacts and improve clinical studies where the current scanning time renders the clinical acquisition

of large regions challenging.

Indeed, XtremeCT-II delivered sharp images and high accuracy for bone morphology and therefore the lack of substantial enhancement is not a surprising outcome. However, a larger improvement may be obtained for other anatomical locations such as the knee joint. Scanning and segmentation of a knee joint is more challenging due to both larger scattering from larger dimensions and stronger partial volume effects because of thinner trabeculae. We hypothesize that for these body parts the benefits of using AT would be more pronounced for XtremeCT-II images as well.

It is important to note that both XTremeCT and XTremeCT-II have a bias and an offset and that values should be corrected to get realistic absolute values. Those bias and offset will however also depend on the used gold standard [21]. Understanding the slope and bias is relatively complex because these depend on multiple factors. For Tb.Sp, we observed a very high slope of the regression line for the standard section (≥ 1.41) for both segmentations. This is because bones with high Tb.Sp tend to have small trabeculae which are not detected by HR-pQCT with either segmentation techniques. For Tb.Th the adaptive thresholding has a low slope. The reason behind this is probably that small trabeculae are more heavily overestimated than thicker trabeculae. ST had a slope closer to 1, but the offset was higher for XTremeCT-II and the correlation was lower.

It is important to note that this study focused only on enhancing the segmentation technique, hence the creation of the gray-value images was not adapted; these were inherently sharper for XtremeCT-II compared to XtremeCT. In a previous study on CBCT images, we have demonstrated that other factors including treatment of the raw projection data, reconstruction and beam hardening correction influence the

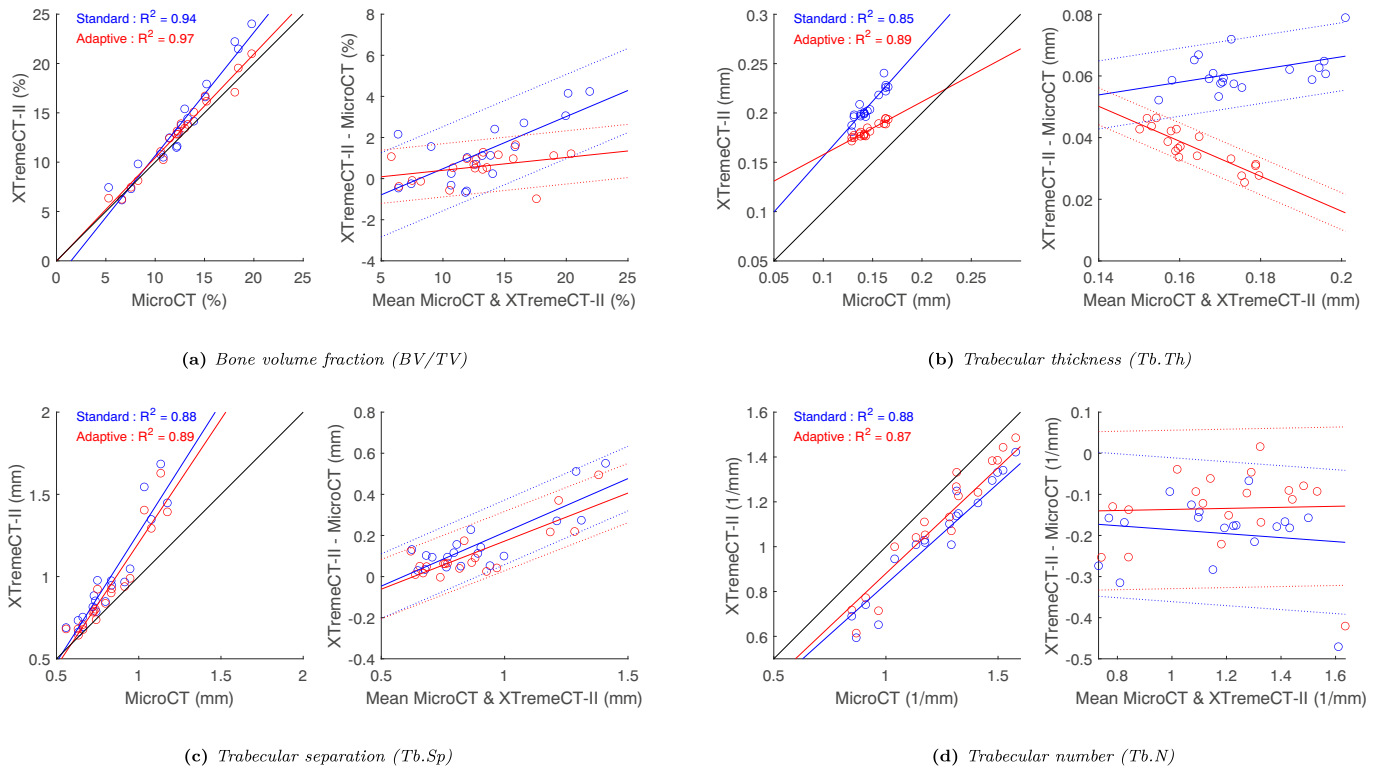


Fig. 4. Scatter plots and Bland Altman plots between MicroCT and XtremeCT-II for the standard region for (a) bone volume fraction (BV/TV), (b) trabecular thickness (Tb.Th), (c) trabecular separation (Tb.Sp) and (d) trabecular number (Tb.N). The XtremeCT-II images were segmented twice: once with the standard software recommended by the manufacturer, referred to as ST, and once with the proposed segmentation technique in this study – adaptive local thresholding – referred to as AT. The solid line on the scatter plot indicates a perfect match with $y = x$.

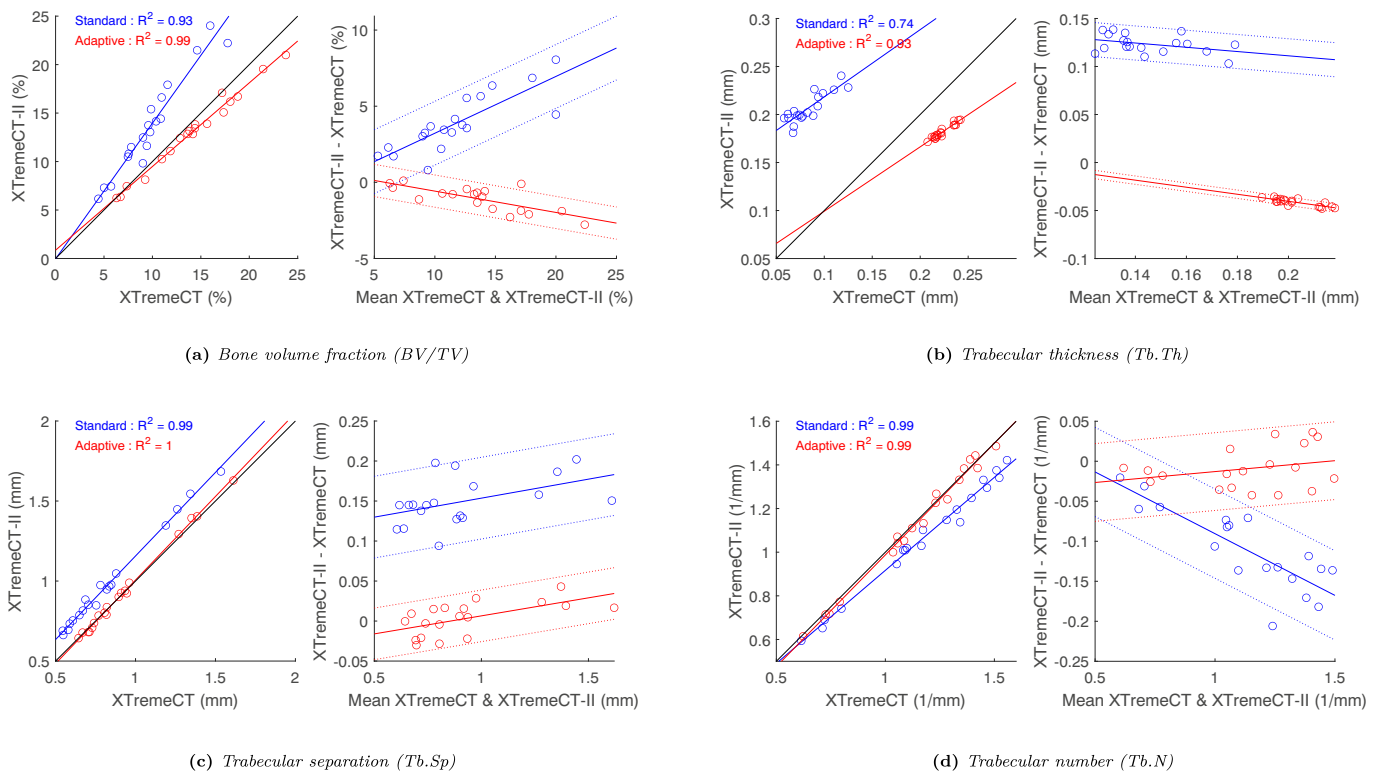


Fig. 5. Scatter plots and Bland Altman plots between XtremeCT-II and XtremeCT for (a) bone volume fraction (BV/TV), (b) trabecular thickness (Tb.Th), (c) trabecular separation (Tb.Sp) and (d) trabecular number (Tb.N). The HR-pQCT images were segmented twice: once with the standard software recommended by the manufacturer, referred to as ST, and once with the proposed segmentation technique in this study – adaptive local thresholding – referred to as AT. The solid line on the scatter plot indicates a perfect match with $y = x$.

Table 2

Agreement between XtremeCT and XtremeCT-II for the standard technique (ST) applying standard segmentation as advised by the manufacturer, and for the segmentation technique proposed in this study using adaptive local thresholding (AT). ** Significant improved from ST to AT at 5%. * Significant improved from ST to AT at 10%.

		ST	AT
Subchondral	BV/TV	0.92**	0.99**
	Tb.Th	0.62**	0.95**
	Tb.Sp	0.97**	0.99**
	Tb.N	0.98*	0.99*
	Average	0.87	0.98
Standard	BV/TV	0.93**	0.99**
	Tb.Th	0.74**	0.93**
	Tb.Sp	0.99**	1.00**
	Tb.N	0.99	0.99
	Average	0.91	0.98
	Average all	0.89	0.98

accuracy significantly. However, investigation of these aspects was out of the scope of the present study.

Burghardt et al. have proposed an adaptive thresholding technique for XtremeCT [22], which however is different from AT proposed in this study. They reported high correlations for all segmentations approaches and analysis techniques which were probably due to the chosen samples, i.e., bone cores from the proximal femur and their results therefore cannot be directly compared with ours. The main drawback of the segmentation technique of Burghardt et al. is that it is relatively complicated, and a lot of parameters should be tuned, which is not the case for our proposed adaptive thresholding technique relying on two parameters.

Limitations of this study include the modest sample size that may not allow generalization of the findings for a larger population. In this study is assumed that the bias and slope are constant and hence, R^2 can be used as accuracy measurement. Larger datasets are needed to confirm this assumption. The thresholds in AT were optimized for the distal radius sections; however, this is also the case for the current ST segmentation of the HR-pQCT scanners. Future studies should investigate the optimal settings for larger sample sets and other anatomical locations. The analyses in this study were limited to trabecular parameters only. Finally, the bones were scanned *ex vivo* and hence the influence of motion artefacts and other detrimental effects arising from surrounding bones and other materials were not considered.

5. Conclusion

The adaptive local thresholding technique can enhance the accuracy of XtremeCT to quantify trabecular bone microstructural parameters close to the XtremeCT-II level for distal radius sections *ex vivo*. It increases the agreement between the two HR-pQCT scanners, which is important for direct comparison of data collected in multicentre studies. For both segmentations and both scanners, the standard section was quantified slightly more accurately compared to the subchondral section.

CRedit authorship contribution statement

Conceptualization: KM, FS, BG, HVL and PV. Methodology: KM, FS, BG, HVL and PV. Software: KM. Validation: KM, FS, BG, CW, JVB, HVL and PV. Formal analysis: KM and PV. Investigation: KM, CW, JVB and PV. Resources: FS, BG, CW, JVB, HVL and PV. Data Curation: KM and PV. Writing – Original Draft: KM. Writing – Review & Editing: KM, FS, BG, CW, JVB, HVL and PV. Visualization: KM. Supervision: FS, HVL and PV. Project administration: FS, HVL and PV. Funding acquisition: FS, HVL and PV.

Declaration of competing interest

All authors state that they have no conflicts of interest.

Acknowledgments

The authors are not compensated and there are no other institutional subsidies, corporate affiliations, or funding sources supporting this study unless clearly documented and disclosed. This research was supported by an FWO travel grant and by KU Leuven Internal Funding (Grant C24/16/027). The authors would like to thank Ursula Eberli (AO Research Institute Davos) for assistance with the IPL software and Dieter Wahl (AO Research Institute Davos) for assistance with the development of scanning techniques and the development of scanner specific holders.

References

- [1] H. Liebl, T. Baum, D.C. Karampinos, J. Patsch, A. Malecki, F. Schaff, E. Ettl, E. J. Rummeny, F. Pfeiffer, J.S. Bauer, Emerging research on bone health using high-resolution CT and MRI, *Curr. Radiol. Rep.* 2 (2014), <https://doi.org/10.1007/s40134-013-0031-y>.
- [2] R. Krug, A.J. Burghardt, S. Majumdar, T.M. Link, High-resolution Imaging techniques for the assessment of osteoporosis, *Radiol. Clin. North Am.* 48 (2010) 601–621, <https://doi.org/10.1016/j.rcl.2010.02.015>.
- [3] X.S. Liu, X.H. Zhang, K.K. Sekhon, M.F. Adam, D.J. McMahon, J.P. Bilezikian, E. Shane, X.E. Guo, High-resolution peripheral quantitative computed tomography can assess microstructural and mechanical properties of human distal tibial bone, *J. Bone Miner. Res.* 25 (2010) 746–756, <https://doi.org/10.1359/jbmr.090822>.
- [4] P. Geusens, R. Chapurlat, G. Schett, A. Ghasem-Zadeh, E. Seeman, J. de Jong, J. van den Bergh, High-resolution in vivo imaging of bone and joints: a window to microarchitecture, *Nat. Rev. Rheumatol.* 10 (2014) 304–313, <https://doi.org/10.1038/nrrheum.2014.23>.
- [5] S.L. Manske, Y. Zhu, C. Sandino, S.K. Boyd, Human trabecular bone microarchitecture can be assessed independently of density with second generation HR-pQCT, *Bone*. 79 (2015) 213–221, <https://doi.org/10.1016/j.bone.2015.06.006>.
- [6] T. Hildebrand, P. Rüeggsegger, A new method for the model-independent assessment of thickness in three-dimensional images, *J. Microsc.* 185 (1997) 67–75, <https://doi.org/10.1046/j.1365-2818.1997.1340694.x>.
- [7] H. Cancellous, B. Microstructural, J.A.N. Dequeker, T.O.R. Hildebrand, A. Laib, R. Mu, Direct Three-Dimensional Morphometric Analysis of, (n.d.).
- [8] Calibration of trabecular bone structure measurements of in vivo three-dimensional peripheral quantitative computed tomography with 28- μ m-resolution microcomputed tomography, *Bone*. 24 (1999) 35–39, [https://doi.org/10.1016/S8756-3282\(98\)00159-8](https://doi.org/10.1016/S8756-3282(98)00159-8).
- [9] A. Laib, P. Rüeggsegger, Comparison of structure extraction methods for in vivo trabecular bone measurements, *Comput. Med. Imaging Graph.* 23 (1999) 69–74, [https://doi.org/10.1016/S0895-6111\(98\)00071-8](https://doi.org/10.1016/S0895-6111(98)00071-8).
- [10] J.A. MacNeil, S.K. Boyd, Accuracy of high-resolution peripheral quantitative computed tomography for measurement of bone quality, *Med. Eng. Phys.* 29 (2007) 1096–1105, <https://doi.org/10.1016/j.medengphy.2006.11.002>.
- [11] S.L. Manske, E.M. Davison, L.A. Burt, D.A. Raymond, S.K. Boyd, The Estimation of Second-Generation HR-pQCT From First-Generation HR-pQCT Using In Vivo Cross-Calibration, *J. Bone Miner. Res.* 32 (2017) 1514–1524, <https://doi.org/10.1002/jbmr.3128>.
- [12] M. Sode, A.J. Burghardt, R.A. Nissenson, S. Majumdar, Resolution dependence of the non-metric trabecular structure indices, *Bone*. 42 (2008) 728–736, <https://doi.org/10.1016/j.bone.2007.12.004>.
- [13] K. Mys, F. Stockmans, E. Vereecke, G.H. van Lenthe, Quantification of bone microstructure in the wrist using cone-beam computed tomography, *Bone*. 114 (2018) 206–214, <https://doi.org/10.1016/j.bone.2018.06.006>.
- [14] K. Mys, P. Varga, B. Gueorguiev, H. Hemmatian, F. Stockmans, G.H. van Lenthe, Correlation between cone-beam computed tomography and high-resolution peripheral computed tomography for assessment of wrist bone microstructure, *J. Bone Miner. Res.* 34 (2019) 867–874, <https://doi.org/10.1002/jbmr.3673>.
- [15] C. de Charry, S. Boutroy, R. Ellouz, F. Duboeuf, R. Chapurlat, H. Follet, J.B. Piat, Clinical cone beam computed tomography compared to high-resolution peripheral computed tomography in the assessment of distal radius bone, *Osteoporos. Int.* 27 (2016) 3073–3082, <https://doi.org/10.1007/s00198-016-3609-4>.
- [16] K. Mys, P. Varga, B. Gueorguiev, V. Neumann, O. Vanovermeire, C.E. Wyers, J.P. W. van den Bergh, G.H. van Lenthe, High-resolution cone-beam computed tomography is a fast and promising technique to quantify bone microstructure and mechanics of the distal radius, *Calcif. Tissue Int.* 108 (2021) 314–323, <https://doi.org/10.1007/s00223-020-00773-5>.
- [17] P. Varga, D.H. Pahr, S. Baumbach, P.K. Zysset, HR-pQCT based FE analysis of the most distal radius section provides an improved prediction of Colles' fracture load in vitro, *Bone*. 47 (2010) 982–988, <https://doi.org/10.1016/j.bone.2010.08.002>.
- [18] T.L. Mueller, D. Christen, S. Sandercott, S.K. Boyd, B. van Rietbergen, F. Eckstein, E.M. Lochmüller, R. Müller, G.H. van Lenthe, B. Van Rietbergen, F. Eckstein, E. Lochmüller, R. Müller, G.H. Van Lenthe, Computational finite element bone mechanics accurately predicts mechanical competence in the human radius of an

- elderly population, *Bone*. 48 (2011) 1232–1238, <https://doi.org/10.1016/j.bone.2011.02.022>.
- [19] H.R. Buie, G.M. Campbell, R.J. Klinck, J.A. MacNeil, S.K. Boyd, Automatic segmentation of cortical and trabecular compartments based on a dual threshold technique for in vivo micro-CT bone analysis, *Bone*. 41 (2007) 505–515, <https://doi.org/10.1016/j.bone.2007.07.007>.
- [20] J.H. Steiger, Tests for comparing elements of a correlation matrix, *Psychol. Bull.* (1980), <https://doi.org/10.1037/0033-2909.87.2.245>.
- [21] K. Mys, P. Varga, F. Stockmans, B. Gueorguiev, C.E. Wyers, J.P.W. Van Den Bergh, G.H. Van Lenthe, Quantification of 3D microstructural parameters of trabecular bone is affected by the analysis software, *Bone*. 142 (2021), 115653, <https://doi.org/10.1016/j.bone.2020.115653>.
- [22] A.J. Burghardt, G.J. Kazakia, S. Majumdar, A local adaptive threshold strategy for high resolution peripheral quantitative computed tomography of trabecular bone, *Ann. Biomed. Eng.* 35 (2007) 1678–1686, <https://doi.org/10.1007/s10439-007-9344-4>.